Supporting Information

Petri et al. 10.1073/pnas.0912295107

SI Text

NMR sample preparation. A fragment of human polycystin-2 identified by limited proteolysis (S1): PC2-EF (N720-P797) was PCR amplified from human PC2 cDNA (obtained from S. Somlo, Yale University), cloned into pET-28 (a+) (Novagen), and transformed into BL21(DE3) CodonPlus RIL (Stratagene) for bacterial expression. Bacteria were grown in either ^{15}N or ^{13}C, ^{15}N-enriched M9 minimal media with 50 μg/mL kanamycin and 30 μg/mL chloramphenicol to $OD_{595} \sim 0.6$ at 37 °C, induced with 1 mM isopropyl-β-D-thiogalactopyranoside and shifted to 30 °C for ∼18 h. Cells were resuspended in Buffer A (20 mM Tris, 500 mM NaCl, pH 8.0), lysed by freeze thaw/sonication with lysozyme (∼1 mg/mL) (Sigma), and clarified by centrifugation (1 h, 20,000 rpms). Supernatant was loaded onto a 1 mL HisTrap column (GE Biosciences). The column was washed with 30 column volumes (CV) Buffer A, then 10 CV Buffer A +50 mM imidazole. Purified PC2-EF was eluted in Buffer A +500 mM imidazole, and applied to a BioRad desalting column equilibrated in 2 mM Tris pH 7.4, 150 mM NaCl, 20 mM $CaCl_2$. PC2-EF was treated with thrombin (1 U/mg) for all experiments to remove the "MGSSHHHHHHSSGLVPRGSHM" tag. Final PC2-EF protein concentration was quantified by Bradford colorimetric protein assay. NMR samples contained the above solution conditions, 1 mM PC2-EF, plus 5% D_2O, 0.05% NaN_3, 10 μM each of PMSF (Sigma), leupeptin, and pepstatin (Calbiochem), and 20 mM Ca^{2+} in order to assure saturation of the Ca^{2+}-bound state.

NMR Spectroscopy. NMR experiments were collected at 30 °C on a Varian INOVA 600 MHz spectrometer and a "room temperature," 5 mm, triple resonance proton-carbon-nitrogen probe equipped with triple-axis (XYZ) pulsed magnetic field gradients (PFGs). NMR spectra were acquired using pulse sequences from the Varian Bio-Pack user library and processed using NMRPipe (S2). Sequential backbone and aliphatic side chain assignments were determined by manual analysis of 2D ^{1}H-^{15}N HSQC (Heteronuclear Single Quantum Coherence), ^{1}H-^{13}C HSQC, and 3D HNCO, HN(CA)CO, HNCACB, HN(CO)CA, HCACO, HCC(CO)NH, ^{15}N-TOCSYHSQC (total correlation spectroscopy), and HCCH-TOCSY NMR experiments collected using ^{13}C, ^{15}N-labeled PC2-EF. Aromatic resonances were assigned using a combination of a 2D ^{1}H-^{13}C HSQC and 3D ^{13}C-NOESYHSQC (Nuclear Overhauser Enhancement Spectroscopy) NMR spectra centered on the aromatic carbons. NMR chemical shift assignments for PC2-EF have been deposited in the BioMagResBank (BMRB accession no. 16590).

Resonance Assignment. ^{1}H, ^{13}C, and ^{15}N NMR chemical shift assignments for PC2-EF were established for nearly all backbone atoms (excepting proline amide ^{15}N nuclei) and a majority of all side chain aliphatic and aromatic resonances. However, most side-chain carboxylate (Glu and Asp), amide (Gln and Asn), amines (Lys), and guanidinium (Arg) groups were not assigned. The 2D ^{1}H-^{15}N HSQC spectrum of PC2-EF collected at 30 °C displayed spectral linewidths and patterns of backbone amide chemical shifts consistent with a folded, all α-helical protein. In this spectrum, nearly all of the expected backbone amide resonances for residues I725-L796 (excepting prolines) were visible and have been labeled, along with the side chain NH2 amides for N720, Q743, Q776, and Q768. Signal-to-noise limitations were overcome by seven-day collections of 3D NOESY-HSQC spectra and the inclusion of residual dipolar couplings (RDC) in structure calculations.

Steady-State $_{1}H \rightarrow {}_{15}N$ NOE Measurements. The relaxation properties of NMR signals are well recognized to depend on local conformational fluctuations of the involved nucleus. The steady-state $^{1}H \rightarrow {}^{15}N$ NOE measured for backbone amide ^{15}N nuclei, indirectly reports on the relative density of localized fast-timescale (nanosecond–picosecond) motions in a residue-specific manner. Pulse sequences for measurement of the steady-state ^{1}H ^{15}N NOE incorporated sensitivity enhancement, water flip-back pulses, and coherence selection via PFGs (S3). The steady-state NOE experiment was performed with and without a 1- or 9-s saturation period to allow buildup of the NOE, and used a total recycle delay of 6 s. Spectral widths of 9 and 2.1 kHz in the f2 and f1 dimensions were set in all experiments, with 128 transients collected.

Measurement and Exponential Fitting of R_1 and R_2 NMR Relaxation Rates. Both T1 and T2 relaxation times were extracted from two series comprising each of ^{1}H-^{15}N HSQC spectra with delays of 100, 300, 500, 700, and 1000 ms for T1 and 10, 30, 70, 150, 190, 250 ms for T2 using SPARKY. Spectra were recorded twice at each time point. Individual increments were separated by a 1-s recycle delay during determination of R_1 and R_2 relaxation rates. NMR peak heights determined by the "rh" command in Sparky were used as reliable indicators of spectral intensity. The program "sparky2rate" (http://xbeams.chem.yale.edu/∼loria/software.htm) read in peak intensity tables from SPARKY and acted as a front-end for Curvefit (http://cpmcnet.columbia.edu/dept/gsas/biochem/labs/palmer/software.html), for exponential fitting of R_1 and R_2 NMR relaxation rates (see Fig. S3) and an analysis of their associated errors using Monte Carlo simulations, which depended upon an initial error estimated from the repeated experiments.

Identification of Dihedral Angle and NOE Distance Restraints. Backbone φ and ψ torsion (dihedral) angle restraints were calculated from patterns of backbone atom chemical shifts using the TALOS (S4) software package. NOE correlations between nearby protons were identified in 3D ^{15}N-NOESY-HSQC and (aromatic) ^{13}C-NOESY-HSQC NMR spectra. All 3D NOESY spectra were extensively analyzed and peak-picked manually using SPARKY (D.G. Kneller and T.D. Goddard, University of California, San Francisco). Interproton distance restraints were interpreted from NOESY peak lists using the automated NOEASSIGN function of the CYANA software package. Following seven iterative rounds of automated NOE peak interpretation, structure determination, and restraint analysis final distance restraints were automatically identified from the NOESY peak lists. TALOS-derived dihedral angle restraints were included throughout the calculations. One manually assigned NOE (between residues L10 of helix α1 and I39 of helix α3), corresponding to a peak in the ^{15}N NOESY spectrum was used, along with residue-specific chemical shift assignments, as input for automated NOESY peak assignment in CANDID/CYANA. NOE constraint lists output by CYANA were then imported to Xplor-NIH for structure calculation and refinement. Assignment of this NOE was unambiguous and supported by automatically assigned structurally adjacent NOEs (i.e., between L10 of α1 and Y43 of α3) in both ^{15}N NOESY and ^{13}C aromatic NOESY spectra. It should be noted that the structure converges without this one manual NOE assignment.

Measurement of Residual Dipolar Couplings. Anisotropic orientational restraints were identified by comparison of total coupling constants (scalar plus residual dipolar) in an NMR sample of similarly Ca^{2+}-saturated, 15N-labeled PC2-EF containing 20 mg/mL of the Pf1 bacteriophage, which was prepared from infection of a 2 L growth of *Pseudomonas aeruginosa*, and compared to an otherwise identical NMR sample lacking the bacteriophage. An additional set of NH RDC constraints were measured in 7% strained polyacrylamide gel using commercially available specialized NMR tube and gel casting chamber (New Era Enterprises, Inc., http://www.newera-spectro.com) for cross-validation of the structure (see Fig. S4). Apparent $^1J_{NH}$ coupling constants were measured using a spin-state-selective 1H, 15N-HSQC NMR pulse sequence (S5), provided as part of the Biopack pulse sequence library.

Tertiary Structure Determination. Tertiary structures for the PC2-EF domain were calculated initially using the NOEASSIGN/CANDID function of the CYANA 2.0 software package (S6, S7) for automated interpretation of NOESY cross-peaks. Final refinement was performed with Xplor-NIH version 2.1 using conformational restraints as detailed below and summarized in Table 1. In the final ensemble of twenty NMR structures, no restraint violation was greater than >0.5 Å for NOE distances, >5° for dihedral angles, or >1 Hz for RDCs, with additional details available in the Table 1. A superposition of backbone traces for the final ensemble has been presented in Fig. 2*A* with a superposition of side chain heavy atoms in Fig. 2*B*. Average rmsds from the mean structure for the backbone atoms were 0.6 Å and, for heavy atoms, were 1.2 Å over the residue range I725-D790. The residue-specific distribution of interresidue NOE restraints and backbone rmsds were compared to the previously described steady-state $^1H \rightarrow {}^{15}N$ NOE values (Fig. 6*A*). Approximately five residues at both termini were structurally disordered as evidenced by a lack of interresidue NOE correlations, decreasing steady-state NOEs, and resultant elevations in residue-specific rmsd values.

NOESY cross-peaks assigned by the CANDID algorithm were converted into distance restraints with upper bounds calibrated based on a reference distance of 5.5 Å and adjusted for nonstereospecifically assigned aromatic, methylene, and methyl protons using the method described originally for DYANA (S6) and detailed in ref. S8. The resulting CYANA-format distance restraints along with the TALOS-derived dihedral angle restraints and RDCs were converted for use in Xplor-NIH. Along with the aforementioned experimental restraints, the Xplor-NIH potential function contains terms for proper covalent geometry, nonbonded violations, empiric volume of gyration, automated hydrogen-bonding potential (HBDB), and RAMA (torsion angle database). The latter two terms have been recognized as required for improved structural accuracy as judged by a number of structural validation servers. Note that, for appropriate molecular packing, expressed both by the Protein Data Bank (PDB) validation server and the MolProbity clash score (S9), the Xplor-NIH parameters for the Xplor potential "VDW" (van der Waals) atom–atom repulsive term was optimized. The Xplor-NIH "refine.py" python script VDW setup statement is as follows: "rampedParams.append(MultRamp(0.9,0.8, "command('param nbonds repel VALUE end end')"))". This statement sets parameters for the Xplor $f_{VDW}(R)$ target function (S16) shown below:

$$f_{VDW}(R)=\left\{\begin{array}{cc}\frac{A}{R^{12}}-\frac{B}{R^6}=4\varepsilon((\frac{\sigma}{R})^{12}-(\frac{\sigma}{R})^6)H(R-R_{cut}) & \text{truncation}\\ (\frac{A}{R^{12}}-\frac{B}{R^6})SW(R,R_{on},R_{off}) & \text{switched}\\ C_{rep}(\max(0,(k^{rep}R_{min})^{irexp}-R^{irexp}))^{rexp} & \text{repel}\end{array}\right\}$$

In refine.py, $f_{VDW}(R)$ is set to the "repel" option, and the "MultRamp(0.9,0.8" term sets values for k^{rep}. According to the authors of Xplor-NIH, this term was optimized to satisfy NOE constraints (S16). Because the attractive term of the $f_{VDW}(R)$ "VDW energy" is turned off in the Xplor repel statement, atoms tend to move further apart during refinement than they would be physically expected. Hence the repel parameter is set by default to $0.9 * R_{min}$ to scale down the repulsive force at the beginning of refinement and allowed to relax to $0.8 * R_{min}$ at the end of refinement (R_{min} is the Van der Waals radius). Although we could refine PC2-EF using default refine.py values with zero violations, structure validation using an external program, MOLPROBITY, revealed van der Waals clashes. To reduce these, while still maintaining zero constraint violations, the Xplor-NIH k^{rep} term was adjusted to "rampedParams.append(MultRamp(0.9,0.86, "command('param nbonds repel VALUE end end')"))". The initial repel parameter is still $0.9 * R_{min}$ as in the default, but only allowed to relax to $0.86 * R_{min}$ instead of $0.8 * R_{min}$ at the end of refinement. All experimental constraints were still satisfied using this refinement protocol, and significant improvements in MOLPROBITY clash scores were observed. The final ensemble of 20 structures with the lowest target function values were selected from a total of 80 independent rounds of structure determination.

Structure Validation. Visualization and graphic rendering of the protein structures for the figures were performed using MOLMOL (S10) and PYMOL (http://www.pymol.org). Atomic coordinates for PC2-EF and structural constraints have been deposited in the Protein Data Bank (PDB ID: 2KQ6). The final ensemble of NMR structures was evaluated by submission to the Protein Structure Validation Software ver. 1.3 (S11), which automates analysis by a suite of structure quality evaluation tools including ProCheck, Prosall, and MolProbity.

Sequence Alignment, Conserved Surface Analysis, and Homology Modeling. The sequence of human PC2-EF (N720-P797) was aligned using the program CLUSTALW (http://www.ebi.ac.uk/Tools/clustalw/) with polycystin-2 and polycystin-2-like-1 (polycystin-L) from a range of eukaryotic species and colored according to the CLUSTAL X scheme using JALVIEW (S12) (Fig. 4*C*). The CLUSTALW sequence alignment was also submitted to CONSURF (S13), which identified possibly functionally important regions on the surface of PC2-EF based on phylogenetic relationships between sequence homologues (Fig. 4*A*). Using the crystal structure of Ca^{2+}-bound human calmodulin (PDB ID: 1CLL), the above alignment and SWISS-MODELLER (http://swissmodel.expasy.org/), we created a homology model of the EF-hand of human polycystin-L. Polycystin-L is closely related to PC2 and appears to contain a C-terminal EF-hand implicated in modulating its channel activity. Our modeling results predict polycystin-L also contains an EF-hand stabilized by a nonstandard HLH motif. The sequence of sea urchin PC2-EF (S14) identified above from the CLUSTALW sequence alignment was submitted to SWISS-MODELLER in "project mode" to create a homology model using the crystal structure of Ca^{2+}-bound human calmodulin (PDB: 1CLL) as a template. The homology model was checked using Swiss-Pdb viewer (S15) and used without further energy minimization (Fig. 4*A*).

1. Celic A, et al. (2008) Domain mapping of the polycystin-2 C-terminal tail using de novo molecular modeling and biophysical analysis. *J Biol Chem* 283(42):28305–28312.

2. Delaglio F, et al. (1995) NMRPipe: A multidimensional spectral processing system based on UNIX pipes. *J Biomol NMR* 6(3):277–293.

3. Farrow NA, et al. (1994) Backbone dynamics of a free and phosphopeptide-complexed Src homology 2 domain studied by 15N NMR relaxation. *Biochemistry* 33(19): 5984–6003.
4. Cornilescu G, Delaglio F, Bax A (1999) Protein backbone angle restraints from searching a database for chemical shift and sequence homology. *J Biomol NMR* 13(3): 289–302.
5. Permi P (2002) A spin-state-selective experiment for measuring heteronuclear one-bond and homonuclear two-bond couplings from an HSQC-type spectrum. *J Biomol NMR* 22(1):27–35.
6. Guntert P, Mumenthaler C, Wuthrich K (1997) Torsion angle dynamics for NMR structure calculation with the new program DYANA. *J Mol Biol* 273(1):283–298.
7. Herrmann T, Guntert P, Wuthrich K (2002) Protein NMR structure determination with automated NOE assignment using the new software CANDID and the torsion angle dynamics algorithm DYANA. *J Mol Biol* 319(1):209–227.
8. Guntert P (1998) Structure calculation of biological macromolecules from NMR data. *Q Rev Biophys* 31(2):145–237.
9. Davis IW, et al. (2007) MolProbity: All-atom contacts and structure validation for proteins and nucleic acids. *Nucleic Acids Res* 35(Web server issue):W375–383.
10. Koradi R, Billeter M, Wuthrich K (1996) MOLMOL: A program for display and analysis of macromolecular structures. *J Mol Graph* 14(1):51–55, 29–32.
11. Bhattacharya A, Tejero R, Montelione GT (2007) Evaluating protein structures determined by structural genomics consortia. *Proteins* 66(4):778–795.
12. Clamp, M., et al., *The Jalview Java alignment editor.* Bioinformatics, 2004. **20**(3): p. 426–7.
13. Landau M, et al. (2005) ConSurf 2005: The projection of evolutionary conservation scores of residues on protein structures. *Nucleic Acids Res* 33(Web server issue): W299–302.
14. Neill AT, Moy GW, Vacquier VD (2004) Polycystin-2 associates with the polycystin-1 homolog, suREJ3, and localizes to the acrosomal region of sea urchin spermatozoa. *Mol Reprod Dev* 67(4):472–477.
15. Guex N, Peitsc MC (1997) SWISS-MODEL and the Swiss-PdbViewer: An environment for comparative protein modeling. *Electrophoresis* 18(15):2714–2723.
16. Brunger AT (1992) *X-plor: Version 3.1 A System for X-Ray Crystallography and NMR*. (Yale University Press, New Haven, CT).

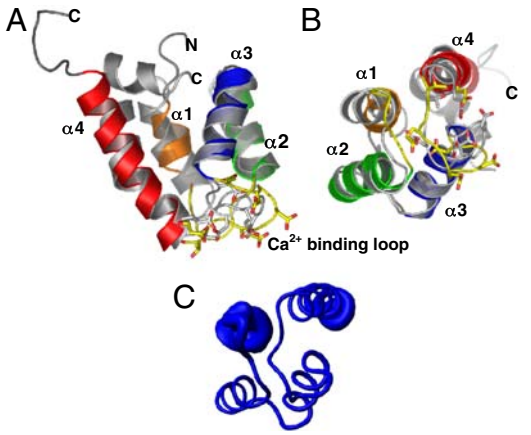

Fig. S1. NMR structure of PC2-EF superimposed with our ROBETTA molecular model of PC2-EF. Coordinates from NMR structure determination of Ca^{2+}-bound PC2-EF (helices α1, α2, α3, and α4 colored orange, green, blue, and red, respectively) were superimposed with the top molecular model (white cartoon) obtained from the ROBETTA De Novo structure prediction server (see http://www.robetta.org/ and ref. S1). Two views are shown (*A*) and (*B*). The NMR structure of PC2-EF has a similar overall secondary structure and 3D conformation compared with the model predicted by the ROBETTA molecular modeling server (rmsd 2.48 Å over residues I725-L789). Some differences are apparent in the α1–α2 loop and in particular in the α2–α3 Ca^{2+}-binding loop [yellow loop, Ca^{2+}-coordinating residues are shown as yellow Corey-Pauling-Koltun (CPK) sticks] likely due to the presence of bound Ca^{2+} in the experimentally determined NMR structure of PC2-EF. (*C*) Sausage representation of the Ca^{2+}-bound PC2-EF NMR ensemble in the same orientation as *B*. Conformational variability is localized to the N terminus, α1-helix, and the C terminus in the top 20 lowest energy conformers of the NMR structure of PC2-EF.

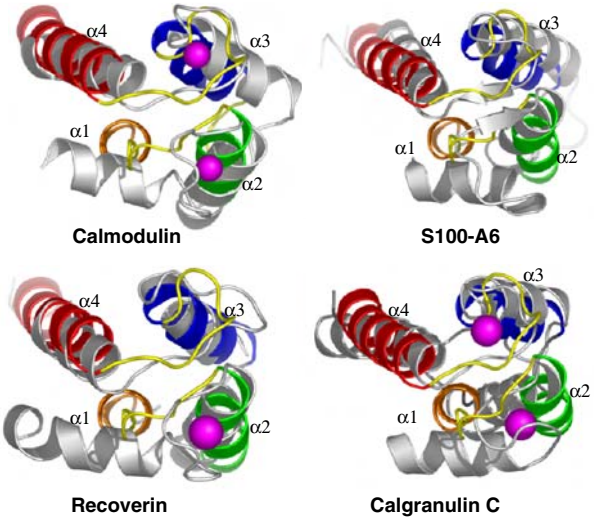

Fig. S2. Structural homologsof the α3–α4 EF-hand in PC2-EF. Structural coordinates for PC2-EF were submitted to the DALI server (http://ekhidna.biocenter.helsinki.fi/dali_server/) (see Table S1). Canonical EF-hands such as calmodulin, S100-A6, recoverin, and calgranulinC were found to be close structural homologs of PC2-EF over helices α3 and α4, whereas α1 and α2 appear to have divergent conformations. In canonical EF-hands, helices corresponding to α1 and α2 are nearly perpendicular, whereas in PC2-EF these helices are approximately parallel to one another. Dali server searches using only PC2-EF α1–α2 as template did not return any EF-hand containing proteins as homologs and the α1–α2 loop does not appear capable of binding Ca^{2+}.

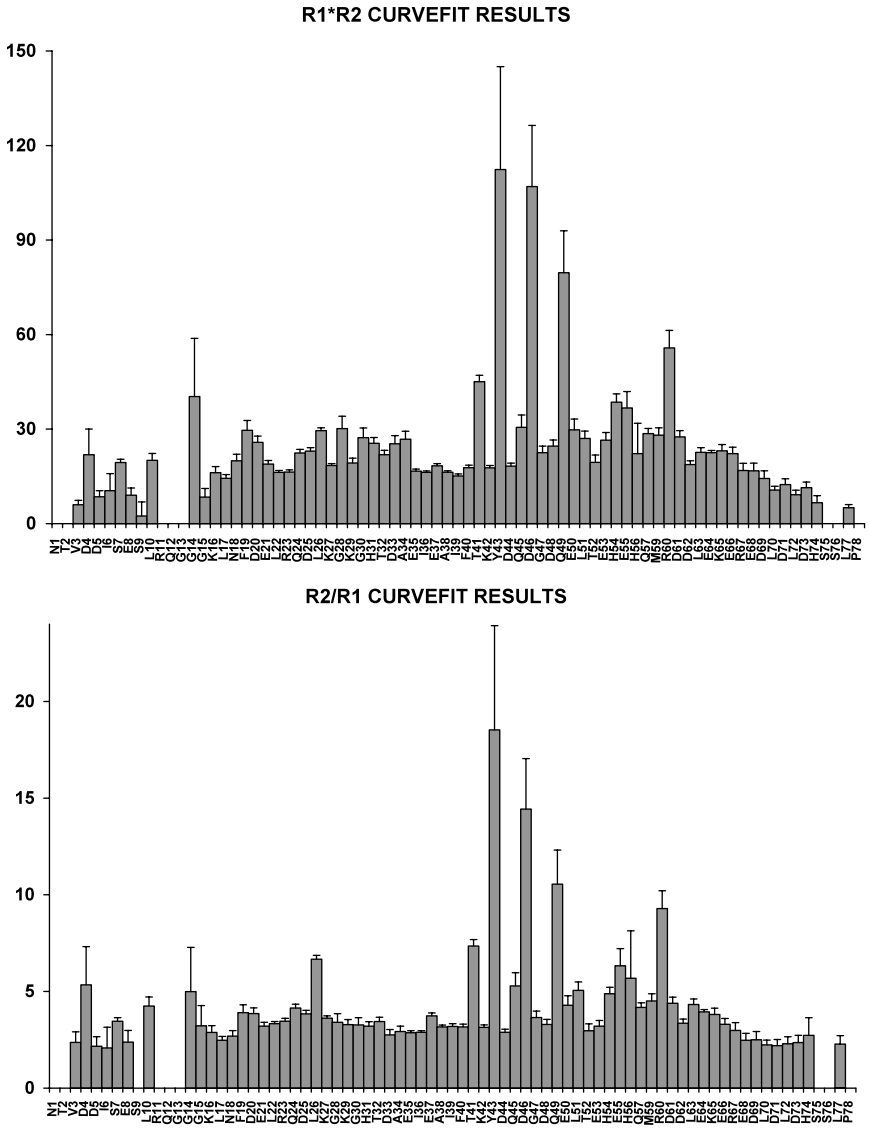

Fig. S3. $R_1 * R_2$ and R_2/R_1 plots for Ca^{2+}-bound PC2-EF. Numerous residues were identified with elevated $R_1 * R_2$ (1) products or R_2/R_1 ratios, and are likely experiencing chemical exchange in agreement with our temperature-sensitive steady-state NOE (Fig. 6) and linewidth measurements. Many of these residues are clustered in the Ca^{2+}-binding loop and we cannot currently distinguish whether the exchange process represents association–dissociation of the bound ligand or whether conformational exchange is present in the complexed state. The average R_2/R_1 value of ~3.5 for ordered residues is consistent with the tumbling rate of a 78-residue, ~9 kDa monomeric protein. The following PC2-EF residues have elevated R_2/R_1 ratios and $R_1 * R_2$ products: D4,L10 (α1 helix), G14 (α1–α2 loop), L26 (α2 helix), T41,Y43 (end of α3 helix), Q45,D46,Q49,E50,L51 (Ca^{2+} binding loop), E55,H56,M59,R60,D61,L63 (α4 helix).

1. Kneller JM, Lu M, Bracken C (2002) An effective method for the discrimination of motional anisotropy and chemical exchange. *J Am Chem Soc* 124(9):1852–1853.

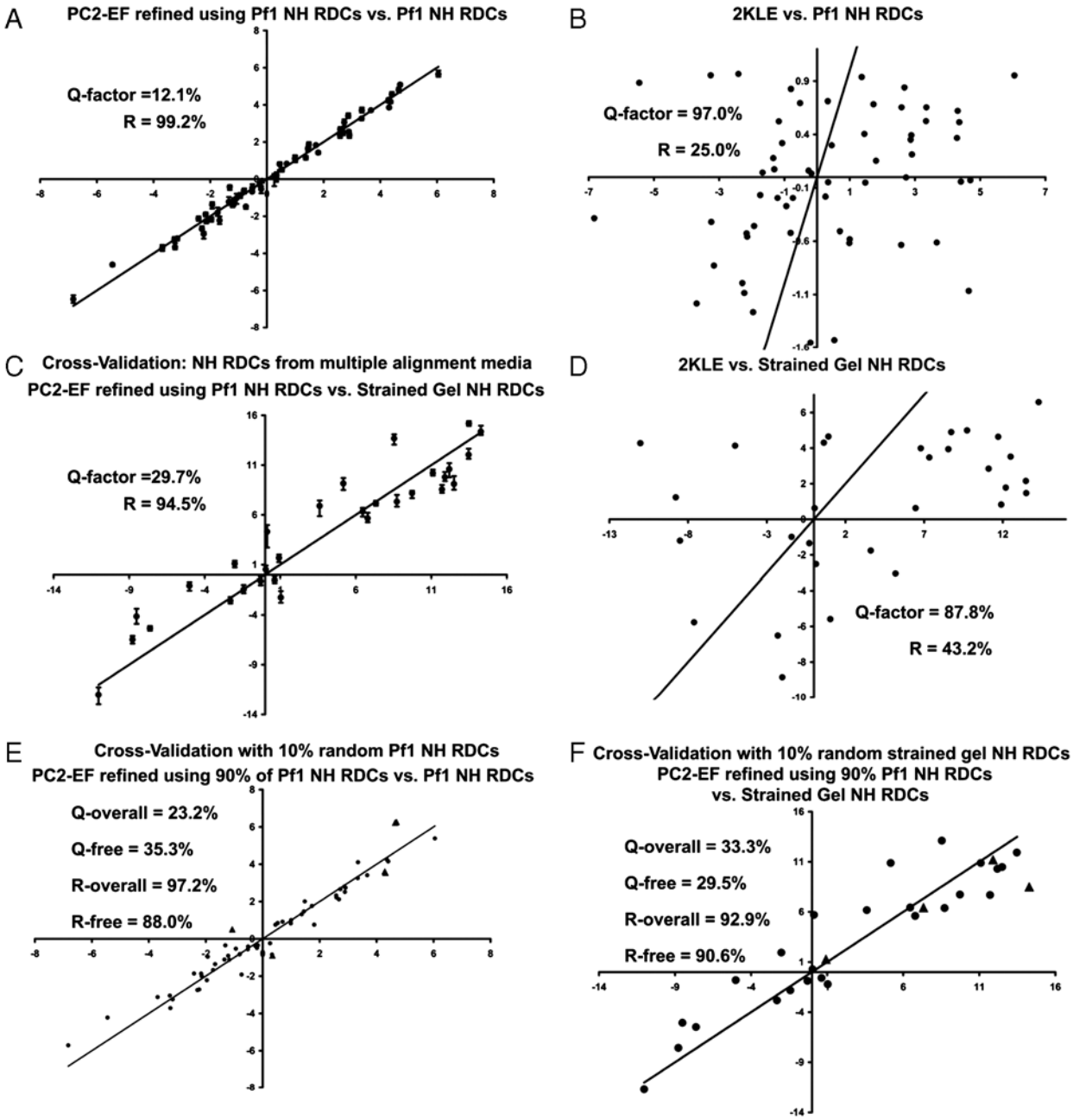

Fig. S4. Cross-validation of the NMR structure of PC2-EF (PDB: 2KQ6) using NH RDCs measured in two alignment media [10 mg/mL Pf1 phage suspension or 7% strained polyacrylamide gel (1)]. The program PALES (2) was used to determine the correlation between experimentally determined RDC values and RDC values back-calculated from structure. Correlation is expressed as both the Q-factor $=$ rms(RDC exp $-$RDCcalc)/rms(RDC exp) and Pearson's R coefficient. (*A*) Correlation between experimentally measured Pf1 NH RDCs and NH RDCs back-calculated from the structure of PC2-EF refined in Xplor-NIH using 59 Pf1 phage derived NH RDC constraints. (*B*) No correlation exists between Pf1 NH RDCs measured on PC2-EF and NH RDCs back-calculated from the structure of 2KLE (3). (*C*) Cross-validation of PC2-EF: Experimental NH RDCs measured in 7% strained polyacrylamide gel (1) correlate with NH RDCs calculated from the structure of PC2-EF refined using Pf1 NH RDCs. (*D*) No correlation between 7% strained polyacrylamide gel NH RDCs measured on PC2-EF and NH RDCs calculated from 2KLE. (*E*) Cross-validation: A randomly selected ~10% subset of Pf1 NH RDCs measured on PC2-EF were left out of an Xplor-NIH refinement of PC2-EF using the remaining 90% Pf1 NH RDCs. This 10% subset Pf1 NH RDCs (▲) were used to calculate a Q-free and R-free for additional cross-validation of the structure of PC2-EF. (*F*) Correlation between strained acrylamide gel NH RDCs measured on PC-2EF and NH RDCs calculated from PC2-EF refined as in *E*. The 10% subset of NH RDCs left out of refinement (▲) were used to calculate Q-free and Pearson's R-free for cross-validation of the structure of PC2-EF.

1. Chou JJ, Gaemers S, Howder B, Louis JM, Bax A (2001) A simple apparatus for generating stretched polyacrylamide gels, yielding uniform alignment of proteins and detergent micelles. *J Biomol NMR* 21:377–382.
2. Zweckstetter M, Bax, A (2000) Prediction of sterically induced alignment in a dilute liquid crystalline phase: aid to protein structure determination by NMR. *J Am Chem Soc* 122:3791–3792.
3. Schumann F, et al. (2009) Ca2+-dependent conformational changes in a C-terminal cytosolic domain of polycystin-2. *J Biol Chem* 284(36):24372–24383.

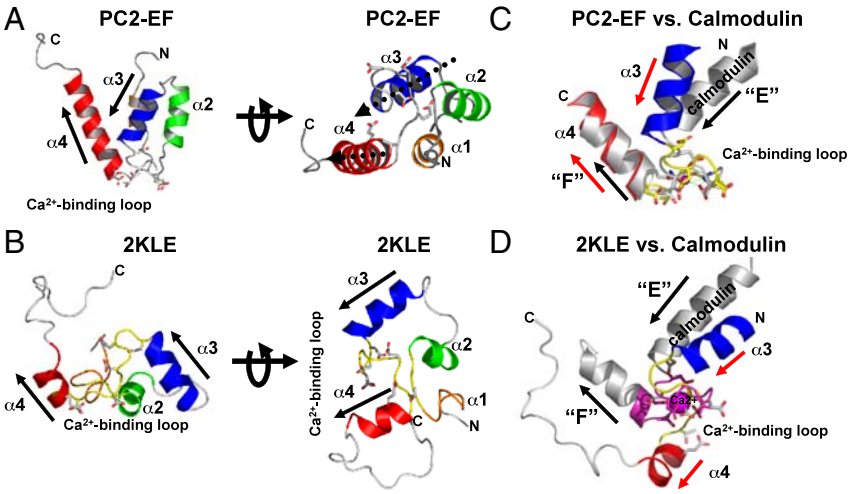

Fig. S5. Structural comparison of PC2-EF and 2KLE. Another NMR structure of the PC2 EF-hand domain (724–796, PDB: 2KLE) (*B*) has been published (1) with a very different fold than the structure of PC2-EF (PDB: 2KQ6) (*A*) presented here. The relative orientation of PC2-EF and 2KLE in each panel (top vs. bottom going left to right) is similar. Helices α1–α4 of PC2-EF and their analogous residues in 2KLE are colored orange, green, blue, and red. In comparison with PC2-EF, 2KLE has secondary structure differences (α1 is missing, α2 and α4 are shorter) and significant backbone and tertiary structure differences. Notably, 2KLE has a flat, planar structure whereas PC2-EF is globular. 2KLE has long interhelical loops and is less compact. In contrast with PC2-EF and calmodulin (*C*), Ca^{2+} binding by 2KLE seems unlikely (*D*) because "E" (α3) and "F" (α4) helices of its EF-hand are parallel, and the α3–α4 interhelical loop has a geometry which positions Ca^{2+}-binding residues in opposing directions. EF-hands have approximately perpendicular "E" and "F" helices and a conserved 12-residue Ca^{2+}-binding loop geometry found in both calmodulin and PC2-EF, but absent in 2KLE.

1. Schumann F, et al. (2009) Ca2+-dependent conformational changes in a C-terminal cytosolic domain of polycystin-2. *J Biol Chem* 284(36):24372–24383.

A WHATCHECK

Z-scores > 0 are better than average
Z-scores < -5.0 indicate structural errors

	2KLE	PC2-EF
1st generation packing	-5.108 (poor)	-1.627
2nd generation packing	-5.177 (bad)	-1.675
Ramachandran plot	-4.492 (bad)	-0.725
Chi-1/chi-2 rotamer	-2.900	1.228
Backbone conformation	-6.563 (bad)	-0.451
Inside/Outside distribution	1.344(unusual)	1.125

B Protein Structure Validation Server

Z-scores > 0 are better than average
Z-scores < -5.0 indicate structural errors

	2KLE	PC2-EF
Procheck G-factor (Φ / Ψ)	-2.87	1.34
Procheck G-factor (all)	-5.03	0.12
MolProbity clashscore	-5.48	0.17
Ramachandran Plot		
Most favored	74.2%	96.7%
Additionally allowed	20.3%	3.3%
Generously allowed	4.7%	
Disallowed	0.8%	

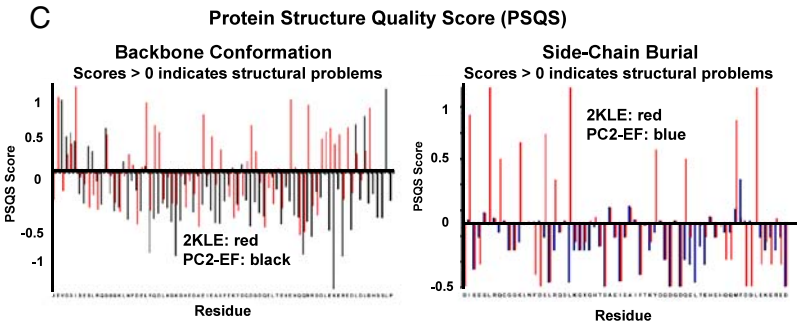

Fig. S6. Structural Validation of 2KLE in Comparison with PC2-EF. The structural coordinates of 2KLE and PC2-EF were analyzed using the protein structure validation software WHATCHECK (*A*) (1), the Protein Structure Validation Server (*B*) (S11), and the Protein Structure Quality Score server (*C*) (2). 2KLE was flagged by WHATCHECK as containing "structural errors" in protein packing and backbone conformation. *Z* scores < – 5.0 in WHATCHECK are listed as likely indicative of an incorrect structural model. The inside/outside distribution of hydrophobic and charged residues in 2KLE was noted as "unusual" by WHATCHECK with a score of 1.34. Normal values for this RMS *Z* score are between 0.84 and 1.16 for globular proteins. Scores >1.2 are associated with proteins containing transmembrane segments, or an atypical pattern of exposed hydrophobic and buried hydrophilic residues. The Protein Structure Validation Server (*B*) found deviations in PROCHECK G factor for dihedral angles and a MOLPROBITY clash score (S9) (a measure of van der Waals clashing) worse than over 90% of proteins tested. The structure 2KLE was found to contain backbone conformation and side chain burial problems across the length of the protein as measured with the Protein Structure Quality Score (*C*). PC2-EF and 2KLE represent very different NMR structure solutions of the EF-hand domain of PC2. The structure of 2KLE was solved with the Intelligent Structure Information Combination (ISIC) method in AUREMOL (3), using another NMR structure (PDB: 1S6I, Ca^{2+}-regulatory region from soybean Ca^{2+}-dependent protein kinase-α) as a template for automated NOESY spectra assignments. Normally, AUREMOL-ISIC uses X-ray structures with high sequence similarity as templates to automate NOESY spectra assignment in a method analogous to molecular replacement in crystallography. However, 1S6I and 2KLE have only ~31% sequence similarity over residues 708–728. Analysis of 1S6I also revealed significant structural geometry errors in WHATCHECK, suggesting that protein geometry problems in 2KLE are due to model bias from the 1S6I template. The structure of PC2-EF (PDB: 2KQ6) scored within the accepted range in all of the above structure validation tests.

1. Hooft RWW, Vriend G, Sander C, Abola EE (1996) Errors in protein structures. *Nature* 381:272.
2. Jaroszewski L, Pawlowski K, Godzik A (1998) Multiple model approach: Exploring the limits of comparative modeling. *J Mol Model* 4:294–309.
3. Schumann F, et al. (2009) Ca2+-dependent conformational changes in a C-terminal cytosolic domain of polycystin-2. *J Biol Chem* 284(36):24372–24383.

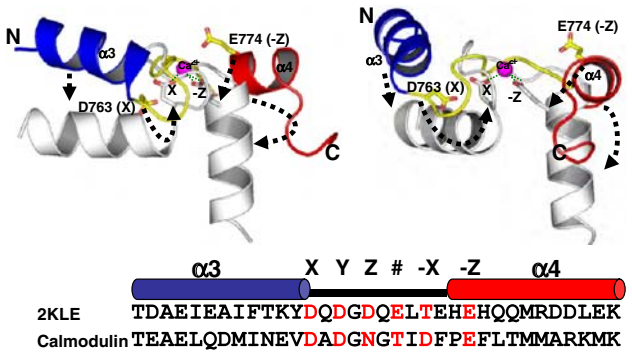

Fig. S7. X and -Z residues in 2KLE have atypical backbone positions and geometry for Ca^{2+}-ligation compared with canonical EF-hands such as calmodulin. During the preparation of this manuscript, another NMR structure of a fragment of PC2 (680–796) encompassing the EF-hand was published (1). This structure, 2KLE, is shown in cartoon format with helices α3 (blue) and α4 (red) and the α3–α4 loop in yellow, aligned with calmodulin (white, PDB ID: 1CLL). Ca^{2+}-coordinating residues in 2KLE at the X and -Z positions are shown as yellow CPK sticks. Ca^{2+}-coordinating residues in calmodulin at the X and -Z positions are shown as white CPK sticks with green dashes indicating coordination bonds with Ca^{2+} (magenta sphere). The predicted Ca^{2+}-binding loop of 2KLE superimposes with the Ca^{2+}-binding loop of calmodulin with an rmsd of ~ 4 Å. Typically the helices in a helix-loop-helix (HLH) EF-hand motif are nearly perpendicular. In 2KLE, α3 is approximately parallel with α4 and the resulting α3–α4 loop geometry appears to prevent D763(X) and E774(-Z) from participating in Ca^{2+} binding. Hypothetical rotations of α3 and α4 which might allow Ca^{2+}-ligation are depicted as dashed arrows.

1. Schumann F, et al. (2009) Ca2+-dependent conformational changes in a C-terminal cytosolic domain of polycystin-2. *J Biol Chem* 284(36):24372–24383.

Table S1. Top EF-hand structural homologs of Ca^{2+}-bound PC2-EF from the DALI server

PDB	*Z* score	rmsd, Å	Aligned	No. residues	Identity, %	Molecule
1cll	3.9	3.7	67	144	18	CALMODULIN
2jtt	3.9	3.3	59	90	24	S100A6
1omr	3.7	3.1	58	201	16	RECOVERIN
1odb	3.5	3.5	61	91	21	CALGRANULIN
1a03	3.5	3.4	60	90	23	CALCYCLIN
1a4p	3.5	3.6	64	92	17	S100A10
1sbj	3.4	2.7	51	81	22	TROPONIN C
1e8a	3.4	3.4	58	87	22	S100A12